Electronic and thermodynamic criteria for the occurrence of high entropy alloys in metallic systems

Electronic and thermodynamic criteria for the occurrence of High Entropy Alloys in metallic systems

M.G Poletti, L. Battezzati
Dipartimento di Chimica, Università degli Studi di Torino, Via Pietro Giuria 7, 10125 Torino.

Abstract

The occurrence of multicomponent solid solutions in multinary metallic systems, also called High Entropy Alloys (HEAs), is classified and predicted by means of both electronic and thermodynamic criteria. Electronic parameters for alloys, i. e. electronegativity, valence electron concentration (VEC), itinerant electron concentration (e/a), are derived and employed together with size mismatch in a scheme akin to Hume-Rothery rules to map HEAs reported in the literature to date. For electronegativity, instead of the usual empirical Pauling scale, the recent Allen scale based on experimental and theoretical data is employed. A thermodynamic approach to the formation of solid solutions in multicomponent systems is then proposed using the regular solution and computing the temperature at which the free energy hypersurface changes curvature at spinodal points. In all cases the maps which have been obtained (electronegativity *vs* size mismatch, VEC *vs* e/a, critical temperature *vs* size mismatch) rank the composition of HEAs according to their phase constitution (solid solutions, solid solution + σ, intermetallics) and can be used all together to improve the formulation of HEAs and predict new ones.

Keywords: High Entropy Alloys, Solid-solution, Hume-Rothery's Rules, Electronegativity, Thermodynamics.

1 Introduction

In the last decade the new family of alloys denominated High Entropy Alloys (HEAs) has raised large interest in metallurgy. Traditionally the search for new alloy compositions was focused on systems based on one main element. A new way of designing alloy compositions was proposed in 2004[1]·[2] by defining for the first time the High Entropy Alloys as those composed of five or more elements in equimolar ratio having simple crystal structure, i. e. solid solutions where solvent and solutes cannot be distinguished. The topic has seen a steady increase of the number of contributions dealing with various aspects of synthesis, processing and determination of properties which are promising in various respects, especially mechanical. A comprehensive review on HEAs [3] as well as general considerations on the metallurgy of HEAs, including the chance of strengthening them by precipitation hardening [4], have just been published.
The thermodynamic stabilization of a solid solution made of several elements in a HEAs is provided by its configurational entropy ΔS^{conf}. This depends on the number of possible ways to arrange N different elements in equimolar ratios in n non-equivalent lattice points of the unit cell, of the solid solution:

$$\Delta S^{conf} = R \cdot \ln N \tag{1}$$

As underlined in [5], considering the different number of n non equivalent lattice points in the unit cell, the solution of *bcc* structure presents the higher configurational entropy up to 5 elements whereas between 5

and 10 elements the fcc has the higher one while the hcp lattice presents ΔS^{conf} greater than bcc and fcc for N higher than 10. It is, therefore, easy to understand how the possible systems to focus on are a huge number. Yeh underlines [2] that, taking equimolar compositions and choosing just 13 metallic elements to form multicomponent systems with 5 to 13 elements, 7099 HEAs are potentially amenable for synthesis. The high number of possible HEAs compositions requires the development of a procedure to predict the formation of a solid solution in such multicomponent equimolar systems. Recently Yang and Zhang [6] proposed a simple parametric model to this purpose employing the enthalpy and entropy of mixing, ΔH_{mix} and ΔS_{mix} respectively, and the radius mismatch between elements. This will be discussed in details below. Takeuchi [7] took a statistical approach for possible candidate compositions of HEAs exploring about 15 million equi-atomic combinations in ΔH_{mix} versus radius mismatch plots where zones for occurrence of either HEAs and bulk metallic glasses (BMGs) were singled out. Otto et *al.* [8] took the deterministic approach of deriving the thermodynamic properties from phase diagram assessment of the ten binaries needed to describe a CoCrFeMnNi quinary HEA. Single elements were then substituted for new alloys (*e.g.* V for Fe) which were synthesized and their phase constitution correlated to the computed differences in free energies between equilibrium states and metastable solid solutions in the respective binaries. Single phased quinary alloys were found in a limited number of cases. The findings were said to cast doubts on the practice of merely mixing several elements to achieve the formation of HEAs. This term was then limited to true solid solutions. The CALPHAD approach was actually employed earlier to evaluate the properties of multicomponent alloys, such as the primary solidified phases or free energy curves of the equilibrium phases, extrapolating data from binary and ternary systems. [9],[10].

In this work we report a thermodynamic approach and the application of Hume-Rothery rules in order to rationalize and predict the formation of HEAs in multicomponent alloys. At first, two-dimensional maps are developed by considering a modern definition of the electronegativity of the elements versus the radius mismatch between them. Then, the occurrence of HEAs is discussed in terms of the total number of both valence and itinerant electrons in the alloy. In the second part of the paper, the thermodynamic treatment proposed by Yang and Zhang [6] is discussed and modified to obtain a new parameter for representing HEAs formation. The outcome of these approaches is verified by analyzing the microstructure of HEAs which were collected from the literature as appeared to date. Note that in a number of papers, the microstructure is reported for the as-cast state. In some cases this may not correspond fully to the equilibrium state of the alloy.

Complex multicomponent systems with more than three elements in high molar fraction have been widely explored in the field of metallic glasses; anyway the Inoue rules [11] for the formation of metallic glasses require thermodynamic and physical properties generally opposite to those needed for the formation of solid solutions: a large negative enthalpy of mixing and a huge radius mismatch. In conventional castings these lead to microstructures composed of mixtures of intermetallic compounds. Rapid solidification is needed to obtain a single glassy phase. For these reasons in this work no glass forming system will be considered.

2 High Entropy Alloys and Hume-Rothery Rules

The Hume-Rothery rules (HRR) have been both invoked and questioned in connection with the occurrence of HEAs. As reported in [12] Hume-Rothery defined 5 factors determining the stability of alloys phases

- an electrochemical effect related to the difference in electronegativity, $\Delta\chi$, of the elements involved,

- a size factor effect related to the difference in the atomic radii of the elements involved,
- atoms of elements near the end of the short periods and those in B subgroups tend to complete their octets of electrons,
- an electron concentration effect stemming from the observation that a definite crystal structure occurs at characteristic numbers of electrons per unit cell, which, if all atomic sites are occupied, is equivalent to saying that similar structures occur at characteristic electrons per atom ratio, e/a, the electron concentration,
- orbital-type restrictions.

For the formation of metallic solid solutions the most important rules to be fulfilled are the first two involving the radius mismatch and the electronegativity while the others are considered when the former are not decisive.

2.1 Hume-Rothery Rules and HEAs: electronegativity and radius mismatch

Guo [13] applied Hume-Rothery rules to HEAs and BMGs together with thermodynamic parameters in order to establish semi-empirically conditions for the formation of either phases. In this work we define two parameters related to the first and second HRR and we verify their ability to predict the formation of a single solid solution phase in multicomponent systems. The first parameter, δ, concerns the atomic radius mismatch [14]:

$$\begin{aligned} \delta &= 100 \cdot \sqrt{\sum_{i=1}^{n} c_i \cdot \left(1 - \frac{r_i}{r_a}\right)^2}, \\ with\ r_i &= radius\, of\, i-th\, element, \\ r_a &= average\, radius \end{aligned} \tag{2}$$

where r_i is the atomic radius of the ith element and r_a is the average atomic radius in the alloy [14]. The second one expresses the difference in electronegativity between elements, $\Delta\chi$:

$$\begin{aligned} \Delta\chi_{Allen} &= 100 \cdot \sqrt{\sum_{i=1}^{n} c_i \cdot \left(1 - \frac{\chi_i}{\chi_a}\right)^2} \\ with\ \chi_i &= electronegativity\, of\, i-th\, element, \\ \chi_a &= average\, electronegativity \end{aligned} \tag{3}$$

where χ_i is the electronegativity of the $i-th$ element [13] and χ_a is the average electronegativity of the elements in the alloy. Instead of the empirical Pauling scale, Allen [15] proposed a new definition of the electronegativy of the elements: it represents the most recent and physically based way to express electronegativity as the average ionization energy of the valence electrons for free atoms in their ground state starting from both theoretical and spectroscopy data. The electronegativity for all *d*-series elements

have become available recently [16]; they are comparable with the Pauling values but with significant differences for some transition metal elements. In this work the electronegativity values from Allen et *al.* [15],[16] are used to evaluate the electrochemical effect in the HEAs systems. Fig.1 shows the location of the alloy compositions listed in Tab.1 in this two parameter space. The multicomponent systems are divided into three categories according to the phase(s) found experimentally in literature: fcc or *bcc* if a single solid solution is formed, SS, where the formation of two solid solutions was evidenced, SS+IM, where an intermetallic phase was obtained, and SS+σ, for systems where the formation of a solid solution and a σ phase occurred. From Fig.1 it is deduced that the HEAs formation can be correlated to HRR using the Allen electronegativity values: there is a clear subdivision in the plot between areas where either solid solutions (*bcc*, fcc, or both) (low lattice mismatch or low electronegativity difference) or IM and σ are obtained. With values of radius mismatch between 1 % and 6 % and $3 > \Delta\chi_{Allen} < 6$, no system forming intermetallic compounds (σ phase included) is located and only solid solutions are formed. In particular, a tendency can be inferred for *bcc* solid solutions to occur at higher radius mismatch and lower electronegativity differences with respect to fcc ones. At higher electronegativity difference, there is a zone where the formation of σ prevails followed by a region where solid solutions plus intermetallic compounds are obtained, probably promoted by high electronegativity differences. In the zone at $\delta \approx 6\%$ and high electronegativity difference, an overlap between solid solution and compounds occurs: it must be noticed in this respect that most of the multicomponent systems appearing here are not equimolar but contain a minority element that very likely promotes intermetallic compounds. The radius mismatch parameter seems to be most relevant in individuating the formation of compounds: at values of δ higher than 6, just intermetallic compounds are experimentally found. These findings show that the simple parameters related to radius and electronegativity differences, although not always decisive, are strongly indicative in the HEAs composition design.

2.2 Hume-Rothery Rules and HEAs: the electronic concentration

HRR recognize that the number of valence (itinerant) electrons per atom, e/a, influences the stability of a given structure, *bcc*, fcc or *hcp*, in solid solutions of noble metal binary systems. Such stabilization depends on the number of electrons per atom because the corresponding Density of States (DoS) present peaks where the Fermi sphere is in contact with the Brillouin zone limit, therefore, at a certain value of the electron concentration a structure is stabilized because more electrons are accommodated in lower energy levels than it would be possible in the levels of another structure. As pointed out by several authors [12], [17] in discussing transition metals not having completely filled d band, the definition of the number of valence electrons per atom (VEC), the fundamental parameter for first principle band calculation which determines the DoS, is not trivial. It is noted that also the enthalpy of mixing, which has been used in the prediction of HEAs formation in [6] and will be in the following, depends on the electron concentration; in fact the d electron band and the heat of formation of an alloy, estimated in [6] by means of the Miedema model, are strictly correlated, as proven by Pettifor [18], who calculated the dependence of the heat of formation of an alloy on the number of d electrons of the metals with a rectangular d band approximation. Guo [17] already individuated a relationship between the total number of electrons, VEC, and the lattice type in the AlCoCrCuFeNi HEAs: a *bcc* structure was related to low values of VEC while fcc lattice appeared at higher VEC values. Recently [19] the formation of the σ phase, classified as electronic phase, has been related in HEAs to the VEC as well.

Here we consider also the influence of the outer s,p electrons to look for a relationship between electronic concentration and solid solution formation in HEAs. Since, as calculated in [20], the cohesive energy

of transition metals is mostly determined by the d-electrons while the s-electron contribution is low, we describe the electronic structure of the transition metal with the Friedel model [21] which considers (i) the electron bands of low momentum, s and p electrons, as a free electron gas having a parabolic density of states starting from ϵ_0, and (ii) a dense, narrower rectangular band formed by d atomic orbitals of width W, centred at the ϵ_d energy as shown in Fig 2. Taking into account the hybridization of the free electron and d bands, the number of effective electrons in the d band, Z_d (weighted occupation of the d-states), depends on the total number of itinerant electron, e/a: Moriarty [22] has found from self-consistent band calculations that if each band state is decomposed into $s-$ and $d-$ like parts, and summed over occupied states, the net occupation, Z_s, of the free electrons band for all transition metals in the $3d$ series is $Z_s = 1.5$. Therefore, as proposed in [21], the effect of hybridization can be taken into account by assuming that the effective number of electrons in the free electron band is $Z_s = 1.5$, so the number of effective electrons in the d-band can be obtained as $Z_d = VEC - Z_s = VEC - 1.5$. As proposed in [21], $Z_s = 1.5$ is used also for the formation of alloys with elements of the $4d$ and $5d$ series. This is applied here in the frame of a rigid band approximation to the description of HEAs electron bands to reveal whether either a single solid solution (bcc or fcc) or intermetallic compounds are formed in multicomponent systems by means of a relationship between the total valence electrons, VEC, and itinerant electrons, e/a, (i. e. the s and p electrons). The HEAs containing more than one solid solution have not been considered because it would not be possible to attribute a definite electronic concentration to any of the two structures. The results for the compositions in Tab. 1 are shown in Fig.3: at VEC > 7.5 and $1.6 < e/a < 1.8$ fcc solid solutions are located while at VEC< 7.5 and $1.8 < e/a < 2.3$ bcc solid solutions are found; the formation of solid solutions plus compounds is located for every VEC number at lower e/a values. From Fig.3 a relationship between the total number of valence electrons, VEC, the number of itinerant electron, e/a, and the structures experimentally found can be argued. Considering the number of s and p electrons in the free electron band equal to $Z_s = 1.5$ we derive that $\epsilon_{s_d} = (e/a) - 1.5$ itinerant electrons are located in the d bands. Decreasing the VEC, the formation of either a bcc or fcc solid solution can occur on increasing the ϵ_{s_d} itinerant electrons transferred from the free electron band to the d-band. At a fixed VEC, lowering the number of e/a electrons means decreasing the number of electrons in the d band and relates to the formation of compounds together with a solid solution. The structure of the alloys reproduces that of pure metals where the bcc phase is stable when the d-band is near half filled while fcc metals present the d-band nearly full. Moreover, as shown in Fig.3, the discrimination between the bcc and fcc structure in HEAs can be related to VEC equal to 7.5, bcc at VEC$<$ 7.5 and fcc for VEC > 7.5; also in this case the similarity with pure metals can be underlined: Pettifor[23], using a calculated density of states based on the construction in Fig. 2, found that, not considering core effects, the stability change between bcc and fcc structure occurs between 7 and 8 valence electrons; HEAs compositions that offer non discrete VEC values are in accordance with these results.

3 Thermodynamic approach

At a given temperature a solid solution between two or more components can occur as equilibrium phase when its free energy of mixing is $\Delta G_{mix} \leq 0$. This is achieved either if $\Delta H_{mix} \leq 0$, being ΔH_{mix} the enthalpy of mixing, or, if ΔH_{mix} is positive but the $-T\Delta S_{mix}$ term, with ΔS_{mix} the entropy of mixing, surmounts it in absolute value. In the latter case, solid solubility becomes complete at all compositions above a critical temperature, T_c. Yang et. al. have defined a further temperature point, T_Z, given by the ratio of ΔH_{mix} to the entropy gain due to the formation of a solid solution, called ΔS^{conf}, to all purposes

identical to ΔS_{mix}, considering the absolute value of ΔH_{mix} calculated by weighing the Miedema enthalpy of mixing of binary systems with respect to concentration:

$$T_Z = \frac{|\Delta H_{mix}|}{\Delta S^{conf}} \tag{4}$$

It is stressed here that, in the case of $\Delta H_{mix} > 0$, this position defines actually a temperature where the free energy of the solid solution equals that of the molar mixture of pure elements in their stable structure, i. e. $\Delta G_{mix} = 0$. Fig. 4 illustrates this for a binary system: the free energy of an equiatomic alloy falls at the maximum of the curve, at the center of the spinodal range. The equilibrium state corresponds, however, to a two phase mixture defined by a common tangent to the two branches of the free energy curve. In the case $\Delta H_{mix} \leq 0$, the above position does not have a thermodynamic meaning for binary alloys (see below for multicomponent systems). Yang [6] *et al.* proposed the Ω parameter:

$$\Omega = \frac{T_m}{T_Z} \tag{5}$$

where T_m is the average of the melting temperature of components, to rank HEAs together with the δ radius mismatch [6] (Eq. 2). In spite of the inaccuracy mentioned above, the Ω parameter provided a successful tool to discriminate between the formation of a solid solution or intermetallics in multicomponent systems. A high value of Ω ($\Omega > 1.1$) and low value of δ ($\delta < 6.6$) correlated to the formation of compact solid solutions in multicomponent alloys.
A rigorous, albeit simple, thermodynamic treatment of the formation of a solid solution for an equiatomic multicomponent system starting from binary interaction parameters is developed in this work. The definition of spinodal points provides a mean to determine a critical temperature, T_{SC}, above which a given alloy is stable as a single homogeneous phase. At T_{SC} the alloy composition coincides with the spinodal point. Here the free energy of mixing as a function of composition changes curvature and its second derivatives become nil. At temperatures higher than T_{SC} the free energy curve has positive curvature expressing the stability of the phase with respect to compositional fluctuations. This composition is still inside the two-phase field since T_{SC} does not coincide with the temperature at which there will be full mixing for the chosen composition, i. e. the binodal hypersurface, however, it must scale with it. Since the calculation of the latter temperature cannot be performed with a simple approach as the one which will be outlined in the following, but would need a full calculation of the multicomponent phase diagram, T_{SC} will be considered here as a critical point above which a single phase can exist.

The free energy of mixing of an N-component system is expressed considering the ideal term containing the entropy of mixing, ΔG^{ideal}_{mix}, and an excess contribution ΔG^{exc}_{mix} due to the non ideal behaviour:

$$\Delta G_{mix}(T,x_A,x_B) \quad = \quad \Delta G_{mix} + \Delta G_{exc} \tag{6}$$

ΔG_{exc} is expressed in the frame of the regular solution model using the binary enthalpy contributions obtained by the Miedema approximation,
[65]$\Delta H^{Miedema}_{mix}$:

$$\Delta G^{ideal}_{mix}(T,x_A,x_B) = RT \cdot \sum_{i}^{N} x_i \cdot lnx_i \tag{7}$$

$$\Delta G^{exc}_{mix} = \sum_{i,j;i>j}^{N} \beta_{i,j} \cdot x_i \cdot x_j \tag{8}$$

$$\beta_{i,j} = 4 \cdot \Delta H^{Miedema}_{mix} \tag{9}$$

The molar fraction of the N-th components is then expressed as $x_N = 1 - \sum_i^{N-1} x_i$, therefore Eqs. 8 and 9 become:

$$\Delta G^{ideal}_{mix}(T,x_A,x_B) = RT \cdot (\sum_{i}^{N-1} x_i \cdot lnx_i \tag{10}$$

$$+ \quad (1 - \sum_{i}^{N-1} x_i) \cdot ln(1 - \sum_{i}^{N-1} x_i))$$

$$\Delta G^{exc}_{mix} = \sum_{i,j;i>j}^{N-1} \beta_{i,j} \cdot x_i \cdot x_j \tag{11}$$

$$+ \quad \sum_{i,N;i>N}^{N} \beta_{i,N} \cdot x_i \cdot (1 - \sum_{i}^{N-1} x_i)$$

(12)

Being the chemical potential of the N-th element a function of all the other (N-1) ones as per the Gibbs-Duhem equation, the composition of a spinodal point can be calculated by setting the determinant D of the Hessian H $(N-1) \times (N-1)$ matrix equal to zero:

$$H(T,x_i,x_j.....x_{N-1}) = \begin{bmatrix} G_{ii} & \dots & G_{i,N-1} \\ \vdots & \ddots & \vdots \\ \vdots & \dots & G_{N-1,N-1} \end{bmatrix}$$

$$det|H| = 0 \tag{13}$$

being G_{ij} and $G_{i,N-1}$ the second and partial derivatives of the free energy of mixing $\Delta G_{mix}(T,x_A,x_B)$:

$$
\begin{aligned}
G_{ii} &= \frac{\partial^2 \Delta G_{mix}(T,x_A,x_B)}{\partial^2 x_i} = RT \cdot (\frac{1}{x_i} \\
&+ \frac{1}{(1-\sum_i^{N-1} x_i)}) - 2 \cdot \beta_{iN} \\
G_{ij} &= \frac{\partial^2 \Delta G_{mix}(T,x_A,x_B)}{\partial x_i \partial x_j} = RT \cdot (\frac{1}{(1-\sum_i^{N-1} x_i)}) \\
&+ \beta_{ij} - \beta_{iN} - \beta_{jN}
\end{aligned}
\tag{14}
$$

The sign of the determinant expresses the stability of an homogeneous system with respect to compositional fluctuations: $D > 0$ means that the homogeneous solution is stable, while $D < 0$ means that it is not. The approximate value for the critical spinodal temperature, T_{SC}, where the determinant D (Eq. 13) changes sign, was found numerically for all multicomponent alloys in Tab.1. The effect of entropy in the stabilization of a homogeneous single phase system can be appreciated by obtaining the value of T_{SC} for a multinary system made of a binary AB alloy with positive interaction parameter to which non interacting components are added in equimolar ratio (interaction parameter $\beta = 0$ J/mol with the A and B elements). Posing $\beta_{AB} = 4000$ J/mol the binary AB has $T_{SC} = 240$ K, a ternary ABC has $T_{SC} = 160$ K, the quaternary ABCD has $T_{SC} = 120$ K and quinary ABCDE has a $T_{SC} = 100$ K.
Also, it should be noted that in a binary system with a negative interaction parameter the singularity of the parameter does not allow a critical temperature because the free energy never changes curvature. On the contrary, in multicomponent systems with all negative but very different interaction parameters, a change in the curvature is possible because of the break of the symmetry of the function: for example in Fig. 5 the free energy ΔG_{mix} of a ternary ABC system with negative interaction parameters ($\beta_{AB} = -1$ J/mol, $\beta_{AC} = -1$ J/mol, $\beta_{BC} = -10000$ J/mol) is shown as calculated at two temperatures (T=40 K and T= 180 K) keeping constant the molar ratio between A and B and adding C. At low temperature the free energy presents both negative and positive curvature, while at T=180 K it has only positive curvature. The value of T_{SC} has been calculated for HEAs compositions and given in Tab. 1. The ratio of the ideal melting temperature of the alloy, T_m, to T_{SC} have then been used to define the μ parameter:

$$
\mu = \frac{T_m}{T_{SC}} \tag{15}
$$

$$
T_m = \frac{\sum_i x_i \Delta H_i^{fusion}}{\sum_i x_i \Delta S_i^{fusion}} \tag{16}
$$

being ΔH_i^{fusion} and ΔS_i^{fusion} the enthalpy and entropy of fusion of the i-th element [67]. Similarly to the Ω parameter proposed by Yang et al. [6], a high value of μ should correspond to the formation of a homogeneous solution in the solid state, whereas $\mu < 1$, should imply that mixing could be possible only at temperatures exceeding the melting point, therefore the alloy should be multi-phased in the solid state.

The μ parameter for the HEAs plotted versus the radius mismatch, δ, is shown in Fig. 6. Each symbol corresponds to a microstructure which was experimentally reported in the literature. For values of δ lower than 3 % the formation of solid solutions occurs, just a single one or a mixture of two. We cannot actually discriminate between *bcc* and fcc phases since the Miedema approach we have adopted provides interaction

parameters for couples of elements irrespective of their structure. In addition, we note there is a tendency to have a single solid solution (squares) at higher μ value with respect two solid solutions (points). At higher value of δ both solid solution mixtures or solid solution plus compounds are formed: in this case lower values of μ correspond to the formation of compounds. The σ phase appears as the main intermetallic compound competing with the formation of solid solutions on increasing both μ and δ. We also recall that the occurrence of a σ phase in several binary systems does not exclude the occurrence of solid solutions to which, actually, the σ phase can transform allotropically [19]. Therefore, the alloys containing σ should be considered with attention in case the multicomponent system where they have been found is of practical interest since the occurrence of such phase could be possibly avoided by proper processing, a practice well developed in processing stainless steels. Also the stability of various other intermetallics can be equalized or surmounted by that of a solid solution because of a favourable entropy term at high temperatures. These phases can then be tailored as hardeners of the matrix, similarly to superalloys [4]. There are inevitable exceptions in Fig. 6: we fully recognize the approximate nature of the present approach as well as the uncertainty in the determination of equilibrium phases in such complex materials, however, the overall picture provides a guideline for the prediction of new HEAs especially when combined with the outcome of the previous paragraph being the electronic approach selective with rescpect to *bcc* and fcc phases.

4 Conclusions

This work proposes a comprehensive approach to understand and possibly predict the occurrence of HEAs, i.e multicomponent metallic solid solution. The Hume-Rothery rules have been applied to several HEAs system finding that:

- the radius and electronegativity mismatch are indicative of the formation of either solid solutions or intermetallic compounds in most multicomponent systems synthesized to date,
- HEAs composition forming either single solid solution or intermetallic compounds have been discriminated considering the contributions of itinerant s and p electrons and the total number of valence electron VEC. Also, the occurence of *bcc* phases solid solution is related to lower VEC and higher e/a with respect fcc,
- a thermodynamic approach based on finding the temperature , T_{SC}, at which the free energy of the solid solution achieves positive curvature, helps in classifying HEAs compositions. In a plot of the ratio of the mixing temperature of the alloy to T_m versus the radius mismatch, regions for the occurrence of solid solutions and intermetallics are clearly outlined.

The combined use of all schemes introduced here can help in indicating when a HEA can be obtained for a given set of elements.

5 Acknowledgments

Prof. M. Chiesa (University of Turin) is acknowledged for discussion on the Allen electronegativity scale. This work has been performed in the frame of the EU-7FP project ACCMET.

Structure	Ref.	Alloys	δ	$\Delta\chi_{Allen}$	μ	e/a	VEC
Compounds	[27]	TiCoCrNiCuAlY	13,29	16,13	0,666	1,86	6,57
Compounds	[27]	$TiCoCrNiCuAlY_{0.8}$	12,6	15,32	0,775	1,85	6,68
Compounds	[27]	$TiCoCrNiCuAlY_{0.5}$	11,17	13,87	0,857	1,85	6,85
Compounds	[28]	AlTiVYZr	10,43	12,32	0,712	2,2	3,8
Ordered BCC + Mo_5Si_3	[29]	AlCrMoSiTi	8,47	11,4	4,691	2,2	4,6
BCC +α	[30]	FeCoCrNiCuAlMo	5,28	9,1	1,093	1,71	7,57
BCC +α	[30]	$FeCoCrNiCuAlMo_{0.8}$	5,23	8,97	1,082	1,74	7,62
BCC + FCC	[30]	$FeCoCrNiCuAlMo_{0.2}$	4,99	8,39	1,153	1,81	7,77
BCC +α	[30]	$FeCoCrNiCuAlMo_{0.4}$	5,09	8,61	1,068	1,78	7,72
BCC +α	[30]	$FeCoCrNiCuAlMo_{0.6}$	5,17	8,8	1,072	1,76	7,67
BCC + Cu+Cr	[27]	TiCoCrNiCuAl	6,58	10,37	1,276	1,83	7,17
BCC + FCC +σ	[31]	$Co_2CrFeNiAlMo_{0.5}$	5,31	7,22	1740,364	1,92	7,39
BCC +σ	[31]	$Co_{1.5}CrFeNiAlMo_{0.5}$	5,78	8,08	17,531	1,92	6,42
BCC +σ	[31]	$Co_{0.5}CrFeNiAlMo_{0.5}$	5,57	7,66	3,465	1,9	6,9
BCC +σ	[32]	$CoCrFe_2NiAlMo_{0.5}$	5,15	7,03	1746,224	1,92	7,23
BCC +σ	[32]	$CoCrFe_{1.5}NiAlMo_{0.5}$	5,32	7,27	1741,336	1,92	7,17
BCC +σ	[32]	$CoCrFeNiAlMo_{0.5}$	5,5	7,53	4,339	1,91	7,09
BCC +σ	[32]	$CoCrFe_{0.6}NiAlMo_{0.5}$	5,65	7,76	5,768	1,9	7,02
BCC + FCC + unknow	[39]	CoCrFeNiCuAlMn	4,6	5,39	1,281	1,86	7,71
BCC + FCC + σ + unknow	[34]	TiCoCrFeNiCuVMn	5,17	9,7	1,583	1,75	7,5
FCC + Laves	[38]	TiCoCrFeNiCu	5,69	10,07	1,226	1,67	8
FCC	[33]	$CoCrFeNiAl_{0.3}Mo_{0.1}$	3,79	5,93	19,862	1,82	7,84
FCC	[38]	$Ti_{0.5}CoCrFeNiCu$	4,5	8,18	1,135	1,64	8,36
FCC + boride	[35]	$CoCrFeNiCuAl_{0.5}B$	14,26	7,07	1,027	1,92	7,46
FCC + boride	[35]	$CoCrFeNiCuAl_{0.5}B_{0.2}$	7,73	5,85	0,994	1,77	8,09
FCC + boride	[35]	$CoCrFeNiCuAl_{0.5}B_{0.6}$	11,75	6,6	0,992	1,85	7,75
FCC + σ	[36]	$Ti_{0.5}Co_{1.5}CrFeNi_{1.5}Mo_{0.5}$	5,12	9,29	6,223	1,75	7,92
FCC + σ	[36]	$Ti_{0.5}Co_{1.5}CrFeNi_{1.5}Mo_{0.8}$	5,3	9,73	5,817	1,71	7,83
BCC + Compounds	[37]	CrFeNiCuZr	10	12,11	1,053	1,6	7,8
BCC+BCC+ Laves	[38]	$Ti_{1.5}CoCrFeNiAl$	6,87	11,01	5,780	1,69	7,69
FCC + Laves	[38]	$Ti_{0.8}CoCrFeNiCu$	5,31	9,42	1,212	1,66	8,14
FCC	[2]	CoCrFeNiCu	1,15	4,5	1,027	1,6	8,8
BCC	[24]	WNbMoTa	2,22	3,77	104,937	1,5	5,5
BCC	[24]	WNbMoTaV	3,23	4,46	6,485	1,6	5,4
BCC+FCC	[37]	MnCrFeNiCu	1,02	4,54	1,002	1,6	8,4
FCC	[41]	$Mn_2CrFeNi_2Cu$	1,07	4,35	1,366	1,71	8,43
BCC+FCC	[41]	$MnCr_2Fe_2NiCu$	0,93	4,75	1,202	1,57	8
FCC	[41]	$Mn_2Cr_2Fe_2Ni_2Cu$	1,04	4,64	1,486	1,67	8,11
BCC+FCC	[41]	$Mn_2CrFe_2NiCu_2$	0,86	3,86	0,860	1,63	8,5
FCC	[41]	$MnCrFe_2Ni_2Cu_2$	1,07	4,03	0,831	1,63	8,88
BCC+FCC	[41]	$Mn_2Cr_2FeNi_2Cu_2$	1,06	4,79	0,977	1,56	8,44
BCC+FCC	[41]	$MnCr_2Fe_2Ni_2Cu_2$	1,06	4,73	0,916	1,56	8,56
BCC+FCC	[49]	$Ti_{0.5}Co_{1.5}CrFeNiAl$	6,05	8,39	5,719	2	7,08
BCC+FCC	[49]	$Ti_{0.5}Co_2CrFeNiAl$	5,94	8,19	6,172	2	7,23
BCC+FCC	[49]	$Ti_{0.5}Co_3CrFeNiAl$	5,71	7,81	6,996	2	7,47
FCC	[42]	$CoCrFeNiCuAl_{0.5}V_{0.2}$	3,9	5,88	1,093	1,74	8,16
BCC+FCC	[42]	$CoCrFeNiCuAl_{0.5}V_{0.4}$	3,93	6,33	1,133	1,75	8,05
BCC+FCC+ σ	[42]	$CoCrFeNiCuAl_{0.5}V_{0.6}$	3,95	6,71	1,175	1,75	7,95
BCC+FCC+σ	[42]	$CoCrFeNiCuAl_{0.5}V_{0.8}$	3,96	7,02	1,219	1,76	7,86
BCC+FCC+σ	[42]	$CoCrFeNiCuAl_{0.5}V$	3,96	7,28	1,265	1,77	7,77
BCC+FCC	[42]	$CoCrFeNiCuAl_{0.5}V_{1.2}$	3,96	7,51	1,293	1,78	7,69
BCC+FCC	[42]	$CoCrFeNiCuAl_{0.5}V_{1.4}$	3,96	7,7	1,352	1,78	7,61
BCC+FCC	[42]	$CoCrFeNiCuAl_{0.5}V_{1.6}$	3,96	7,86	1,394	1,79	7,54
BCC+FCC	[42]	$CoCrFeNiCuAl_{0.5}V_{1.8}$	3,95	8	1,437	1,8	7,47
BCC+FCC	[42]	$CoCrFeNiCuAl_{0.5}V_2$	3,94	8,12	1,481	1,8	7,4
FCC + Compounds	[37]	MoCrFeNiCu	4,13	8,8	0,824	1,4	8,2

Structure	Ref.	Alloys	δ	$\Delta\chi_{Allen}$	μ	e/a	VEC
FCC	[48]	$Ti_{0.5}CoCrFeNiCu_{0.75}Al_{0.25}$	5,07	8,35	1,385	1,73	8
FCC+BCC	[48]	$Ti_{0.5}CoCeFeNiCu_{0.5}Al_{0.5}$	5,51	8,47	1,851	1,82	7,64
BCC1+BCC2	[48]	$Ti_{0.5}CoCrFeNiCu_{0.25}Al_{0.75}$	5,87	8,56	3,005	1,92	7,42
BCC+BCC	[45]	$Ti_{0.5}CoCrFeNiCu_{0.25}Al$	6,05	8,51	3,030	1,96	7,09
BCC+BCC	[45]	$Ti_{0.5}CoCrFeNiCu_{0.5}Al$	5,95	8,43	1,933	1,92	7,25
FCC	[46]	$Ti_{0.2}CoCrFeNiCuAl_{0.5}$	0,21	6,74	1,092	0,09	0,34
BCC+FCC	[46]	$Ti_{0.4}CoCrFeNiCuAl_{0.5}$	0,21	7,8	1,165	0,09	0,36
BCC+FCC	[46]	$Ti_{0.6}CoCrFeNiCuAl_{0.5}$	0,21	8,64	1,212	1,75	7,85
BCC+FCC+σ	[46]	$Ti_{0.8}CoCrFeNiCuAl_{0.5}$	5,81	9,33	1,241	1,76	7,73
BCC+FCC+σ	[46]	$TiCoCrFeNiCuAl_{0.5}$	6,06	9,9	1,286	1,77	7,62
BCC+FCC+σ	[46]	$Ti_{1.2}CoCrFeNiCuAl_{0.5}$	6,27	10,39	1,332	1,78	7,51
BCC+FCC+Comp.	[46]	$Ti_{1.4}CoCrFeNiCuAl_{0.5}$	6,44	10,81	1,371	1,78	7,41
BCC+FCC+Comp.	[46]	$Ti_{1,6}CoCrFeNiCuAl_{0.5}$	6,58	11,17	1,422	1,79	7,31
BCC+FCC+Comp.	[46]	$Ti_{1.8}CoCrFeNiCuAl_{0.5}$	6,69	11,48	1,464	1,8	7,22
BCC+FCC+Comp.	[46]	$Ti_2CoCrFeNiCuAl_{0.5}$	6,79	11,76	1,508	1,8	7,13
BCC	[9]	$MnCrFe_{1.5}Ni_{0.5}Al_{0.3}$	3,32	4,6	3,776	1,84	7,19
BCC	[9]	$MnCrFe_{1.5}Ni_{0.5}Al_{0.5}$	4,03	4,79	3,670	1,89	7
FCC	[43]	$CoCrFeNiAl_{0.25}$	3,31	5,3	1,772	1,82	7,94
FCC	[43]	$CoCrFeNiAl_{0.375}$	3,85	5,47	1741,122	1,86	7,8
FCC+BCC	[43]	$CoCrFeNiAl_{0.5}$	4,27	5,62	2,854	1,89	7,67
FCC+BCC	[43]	$CoCrFeNiAl_{0.75}$	4,87	5,85	5,534	1,95	7,42
FCC+BCC	[43]	$CoCrFeNiAl_{0.875}$	5,1	5,95	1636,575	1,97	7,31
BCC	[43]	$CoCrFeNiAl_{1.25}$	5,59	6,16	1574,347	2,05	7
BCC	[43]	$CoCrFeNiAl_{1.5}$	5,8	6,26	1538,637	2,09	6,82
BCC	[43]	$CoCrFeNiAll_2$	6,08	6,38	1477,950	2,17	6,5
BCC	[37]	$CoCrFeNiAl_{2.5}$	6,23	6,43	1428,318	2,23	6,23
BCC	[37]	$CoCrFeNiAl_3$	6,29	6,44	1386,972	2,29	6
FCC	[43]	CoCrFeNi	1,18	4,85	10,236	1,75	8,25
FCC	[28]	CoFeNiCuV	2,78	7,17	1,103	1,8	8,6
BCC+FCC	[1]	CoCrFeMnGeNi	0,99	5,76	3,747	2	9,17
FCC	[1]	CoCrFeMnCuNi	1,05	4,28	1,195	1,67	8,5
FCC	[1]	CoCrFeMnNi	1,06	4,46	7,384	1,8	8
BCC	[28]	$CoCrFeNiCu_{0.25}Al$	5,18	5,98	2,912	1,95	7,38
FCC	[47]	$CoCrFeNiCu_{0.25}Al_{0.75}$	3,05	5,04	1,244	1,7	8,4
fCC	[47]	$CoCrFeNiCu_{0.5}Al_{0.5}$	1.12	5,46	1,691	1,8	8
BCC+FCC	[47]	$CoCrFeNiCu_{0.75}Al_{0.25}$	4,76	5,79	2,936	1,9	7,6
FCC	[2]	$CoCrFeNiCuAl_{0.3}$	3,19	5,04	1,042	1,68	8,47
FCC	[2]	$CoCrFeNiCuAl_{0.5}$	20.38	5,31	1,053	1,73	8,27
BCC+FCC	[2]	$CoCrFeNiCuAl_{0.8}$	4,55	5,63	1,072	1,79	8
BCC+FCC	[2]	CoCrFeNiCuAl	4,87	5,8	1,090	1,83	7,83
BCC+FCC	[2]	$CoCrFeNiCuAl_{1.3}$	5,24	6	1,111	1,89	7,6
BCC+FCC	[2]	$CoCrFeNiCuAl_{1.5}$	5,43	6,1	1,127	1,92	7,46
BCC+FCC	[2]	$CoCrFeNiCuAl_{1.8}$	5,65	6,23	1,156	1,97	7,27
BCC+FCC	[2]	$CoCrFeNiCuAl_2$	5,76	6,3	1,178	2	7,14
BCC	[2]	$CoCrFeNiCuAl_{2.3}$	5,9	6,38	1,206	2,04	6,97
BCC	[2]	$CoCrFeNiCuAl_{2.5}$	5,97	6,42	1,223	2,07	6,87
BCC	[2]	$CoCrFeNiCuAl_{2.8}$	6,05	6,47	1,247	2,1	6,72
BCC	[2]	$CoCrFeNiCuAl_3$	6,09	6,5	1,269	2,13	6,63
BCC+BCC	[53]	CoCrFeNiCuAlSi	6	6	1,254	2,14	7,29
BCC+FCC	[53]	CoCrNiCuAl	5,29	6,34	1,048	1,81	7,77
BCC	[54]	$CoCrNiCu_{0.5}Al$	5,52	6,49	1,579	1,89	7,44
BCC + FCC	[54]	TiCoCrFeNiCuAlV	5,9	9,92	1,025	1,88	7
BCC	[55]	MnCrFeNiCuAl	4,77	5,59	1,071	1,83	7,5
BCC1+BCC2	[51]	TiCoCrFeNiAl	6,61	10,06	5,241	2	6,67
BCC+Cu+Cr	[27]	TiCoCrCuNiAl	6,58	10,37	1,264	1,83	7,17
FCC	[50]	$Ti_{0.1}CoCrFeNiAl_{0.3}$	4,11	6,31	8,021	1,84	7,8

Structure	Ref.	Alloys	δ	$\Delta\chi_{Allen}$	μ	e/a	VEC
BCC+FCC	[52]	$TiCr_{0.5}FeNiCuAl$	6,53	10,53	1,086	1,91	7,09
BCC+FCC	[52]	TiCrFeNiCuAl	6,36	10,14	1,126	1,83	7
BCC+FCC	[52]	$TiCr_{1.5}FeNiCuAl$	6,2	9,79	1,189	1,77	6,92
BCC+FCC	[52]	$TiCr_2eNiCuAl$	6,05	9,47	1,245	1,71	6,86
BCC+FCC	[52]	$TiCr_3FeNiCuAl$	5,77	8,92	1,233	1,63	6,75
SS+Laves	[63]	CrNbTiZr	7,84	8,72	4,063	1,5	4,75
SS+Laves	[63]	CrNbTiVZr	7,72	8,09	5,303	1,6	4,8
BCC	[63]	NbTiVZr	6,18	5,42	4,157	1,75	4,5
BCC	[63]	$NbTiV_2Zr$	6.58	5,83	5,089	1,8	4,6
BCC	[6]	NbTiVTaAl	3,23	6,97	5,420	2	4,4
BCC	[6]	$NbTiVTaAl_{0.5}$	3.40	6,35	5,821	1,89	4,55
BCC	[6]	$NbTiVTaAl_{0.25}$	3,5	5,82	5,621	1,82	4,65
BCC	[6]	NbTiVTa	3,61	5,01	8,465	1,75	4,75
BCC+FCC+Comp.	[8]	TiCrFeMnNi	6,05	10,22	6,475	1,8	7
BCC+FCC	[8]	CoCrFeMnCu	0,85	4,11	1,000	1,6	8,2
BCC+FCC+CuSn	[64]	$FeCoCuNiSn_{0.5}$	8,69	1,5	1,030	2	10
FCC	[64]	$FeCoCuNiSn_{0.07}$	3,82	1,75	0,948	1,79	9,58
Compounds	[28]	ZrTiVCuNiBe	11,42	13,42	1,711	1,5	5,67
Compounds	[28]	$Ti_2CoCrFeNiCu$	6,73	12,09	1,491	1,71	7,43
Compounds	[61]	ZrHfTiCuFe	9,81	18,23	1,433	1,8	5,8
Compounds	[61]	ZrHfTiCuCo	10,21	18,73	2,124	1,8	6
Compounds	[8]	CoMoFeMnNi	4,45	8,32	1,218	1,8	8
SS+ σ	[8]	CoCrVMnNi	2,83	7,38	7,085	1,8	7,4
SS $+\sigma$	[8]	CoVFeMnNi	2,83	6,98	5,263	1,8	7,4
BCC + FCC	[17]	$FeCrCuAl_{0.2}$ Ni_2	2,8	5,14	1,024	1,65	8,77
BCC + FCC	[17]	$FeCrCuAl_{1.2}$ Ni_2	5,19	6,22	1,048	1,87	7,84
BCC + FCC	[17]	$FeCrCuAlNi_2$	4,93	6,08	1,061	1,83	8
BCC+FCC	[56]	$Co_{0.5}CrFeNiCuAl$	4,97	5,95	0,989	1,82	7,73
BCC+FCC	[56]	$CoCr_{0.5}FeNiCuAl$	5,08	5,62	1,027	1,91	8
BCC+FCC	[56]	$CoCrFe_{0.5}NiCuAl$	5,06	6,04	1,048	1,82	7,82
BCC+FCC	[56]	$CoCrFeNi_{0.5}CuAl$	4,94	5,78	0,971	1,82	7,64
BCC	[56]	$CoCrFeNiCu_{0.5}Al$	5,07	5,92	1,767	1,91	7,55
BCC+FCC	[53]	CoCuNiAl	5,83	5,93	1,036	2	8,25
FCC	[54]	$CoCrFeNiCu_{0.5}$	1,17	4,67	1,621	1,67	8,56
BCC1+BCC2+FCC	[39]	TiCoCrFeNiCuAl	6,28	9,73	1,315	1,86	7,29
BCC+FCC	[39]	VCoCrFeNiCuAl	4,7	7,33	1,298	1,86	7,43
BCC1+BCC2	[48]	$Ti_{0.5}CoCrFeNiCu_{0.2}5Al_{0.75}$	5,87	8,56	2,993	1,91	7,27
FCC	[36]	$Ti_{0.5}Co_{1.5}CrFeNi_{1.5}Mo_{0.1}$	4,77	8,5	7,421	1,8	8,05
FCC	[33]	$CoCrFeNiMo_{0.3}$	2,96	7,62	21,375	1,7	8,09
BCC + FCC + unknow	[39]	CoCrFeNiCuAlMn	4,6	5,39	1,281	1,86	7,71
FCC+AuCu	[66]	CoCrFeNiCuAlAu	6,23	6,52	0,787	1,67	8,33
FCC	[38]	$Ti_{0.5}CoCrFeNiCu$	4,5	8,18	1,142	1,64	8,36
BCC+BCC	[51]	$Ti_{0.5}CoCrFeNiAl$	6,15	8,59	5,320	2	6,91
BCC	[51]	CoCrFeNiAl	5,29	6,03	1614,533	2	7,2
FCC	[33]	$CoCrFeNiTi_{0.3}$	4,11	7,62	8,744	1,7	8,09
BCC	-	CoFe	0,87	1,1	1789,027	2	8,5
BCC	-	MoV	1,97	2	2572,536	1,5	5,5
FCC	-	FeNi	1,12	2,17	1765,088	2	9
FCC	-	CoNi	0,24	1,08	1746,309	2	9,5

Table 1. Compositions and relevant data for HEAs.

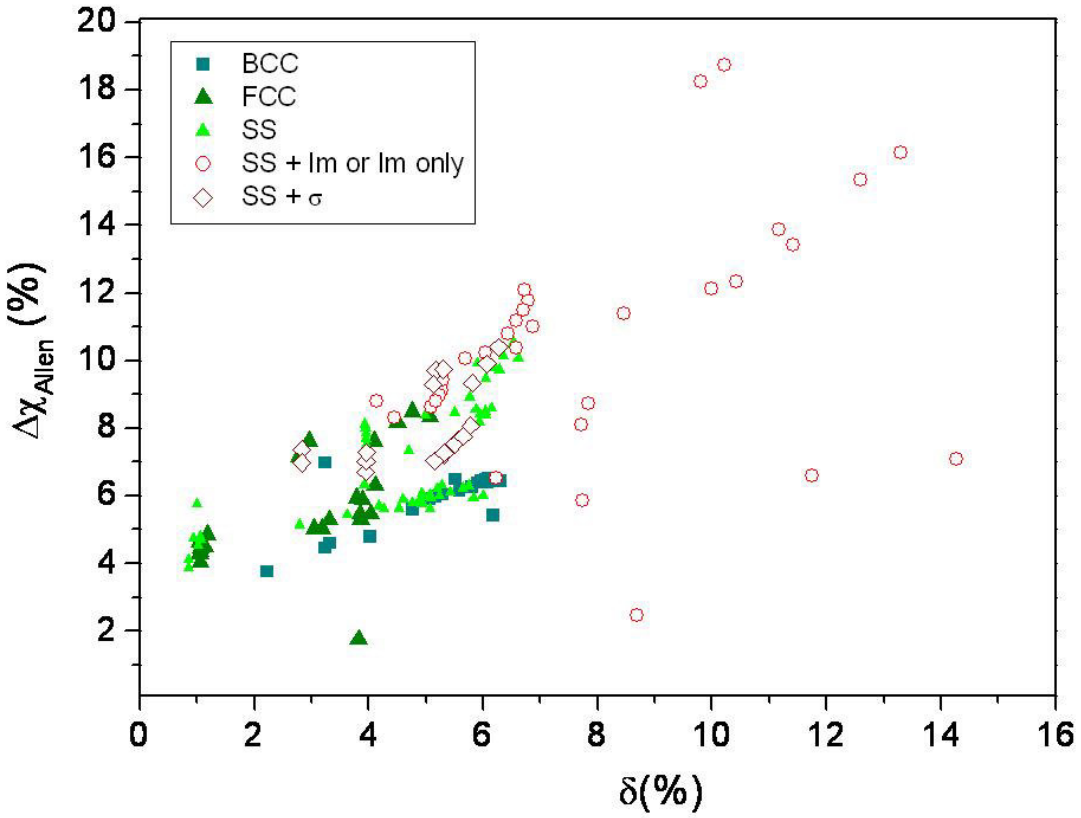

Figure 1. Radius versus electronegativity mismatch for the multicomponent systems listed in Tab 1. BCC and FCC stands for formation of only one phase, SS stands for formation of more solid solutions, SS + IM for formation of solid solution and compounds or only compounds, SS + σ for systems where the formation of solid solution plus σ phase occurs.

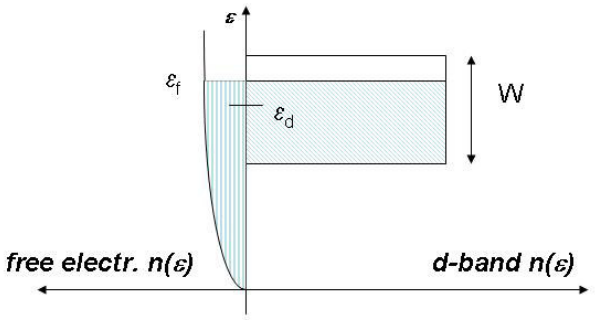

Figure 2. Friedel model for the electronic band of transition metal. The DoS is subdivised in a free electron and a d band. ϵ_f is the Fermi energy, ϵ_d the energy corresponding to the center of the d band, W the width of the d band.

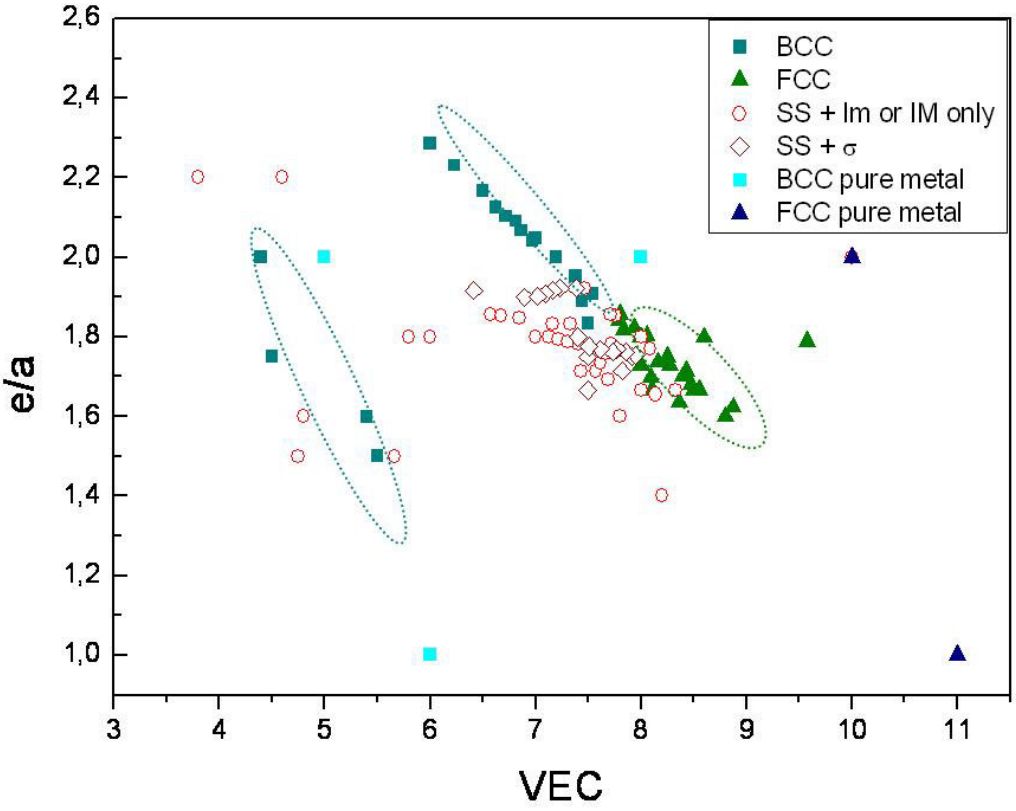

Figure 3. Total number of valence electrons per atom, VEC, versus itinerant electrons per atom, e/a, for different multicomponent systems (Tab. 2.2) forming solid solutions or intermetallic compounds. Legend as in Fig. 1 with the addition of squares and triangles showing the position of pure elements in the plot. The ellipses indicate the zone where different structures are experimentally found. The VEC and e/a values for the *bcc* and fcc pure metals are: at $VEC = 6$ and $e/a = 1$ there is *bcc* Cr, at VEC=8 and $e/a = 2$ respectively *bcc* Fe is located, at $VEC = 10$ and $e/a = 2$ fcc Ni is found and fcc Cu for VEC=11 and e/a=1. The values of VEC and e/a for the binary systems forming a *bcc* or fcc solid solution at 50% at., as CoFe and MoV (*bcc*), FeNi and CoNi (fcc) fall close to the electronic concentration of the multinary systems with the same structure (Tab.1).

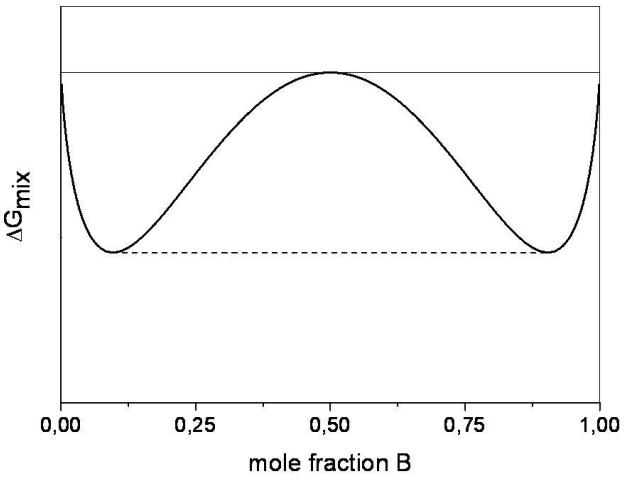

Figure 4. (a) The free energy of mixing ΔG_{mix} calculated with the regular solution model for an alloy having $\Delta H_{mix} > 0$ at the temperature where $\Delta G_{mix}(0.5) = 0$

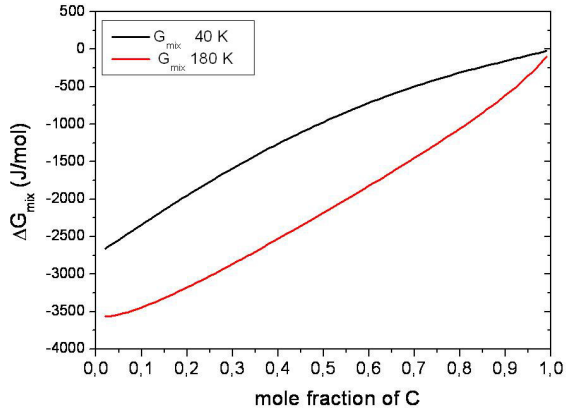

Figure 5. Free energy of mixing ΔG_{mix} of a ternary ABC system with $\beta_{AB} = -1\ J/mol$, $\beta_{AC} = -1\ J/mol$, $\beta_{BC} = -10000\ J/mol$ for T=40 K and T= 180 K.

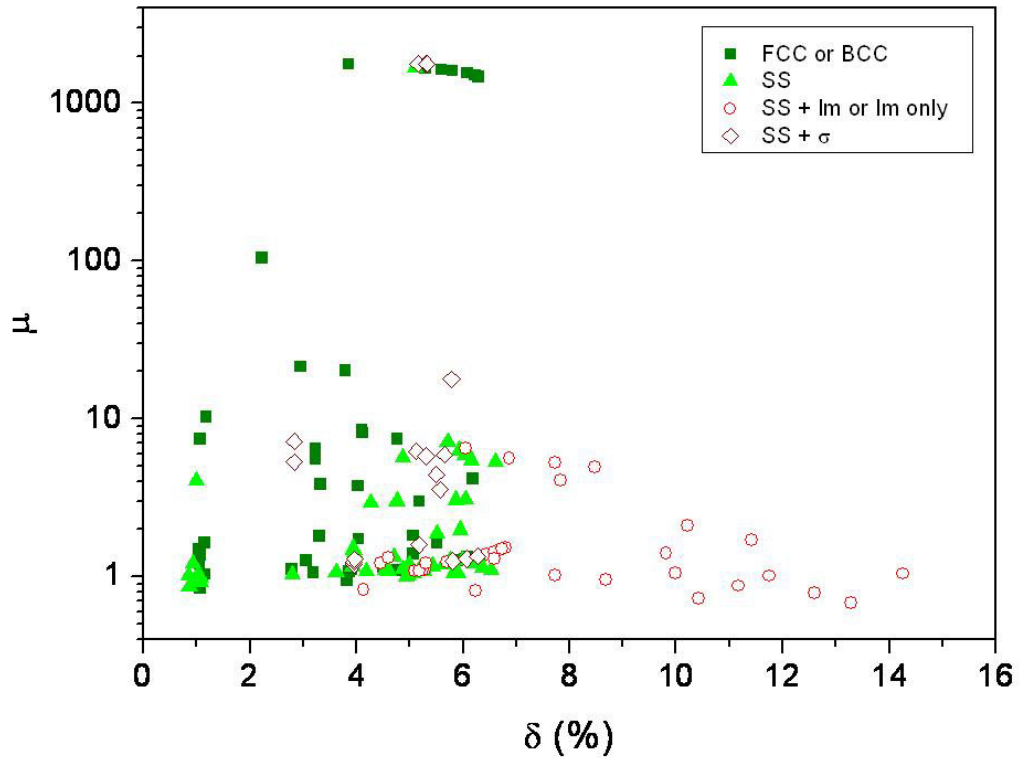

Figure 6. μ parameter versus δ radius mismatch for the alloys listed in Tab.1. Legend as in Fig. 1

Bibliography

[1] Cantor B, Chang ITH, Knight P, Vincent AJB. Mater Sci Eng A 2004;375:213.
[2] Yeh JW, Chen SK, Lin SJ, Yiew J, Chin TS, Shun TT, Tsai CH, Chang SY. Adv Eng Mater 2004;6:299.
[3] Zhang Y, Zuo TT, Tang Z, Gao MC, Dahmen KA, Liaw PK, Lu ZP. Prog Mater Sci 2014;61:1.
[4] Miracle DB, Miller JD, Senkov ON, Woodward C, Uchic MD, Tiley J. Entropy 2014; 16:494.
[5] Cunliffe A, Plummer J, Figueroa I, Todd I. Intermetallics 2012;23:204.
[6] Yang X, Zhang Y. Mater Chem Phys 2012;132:233.
[7] Takeuchi A, Amiya K, Wada T, Yubuta K, Zhang W, Makino A. Mater Trans 2014;55:165.
[8] Otto F, Yang Y, Bei H, George EP. Acta Mater 2013;61:2628.
[9] Hsieh KC, Yu CF, Hsieh WT, . Chiang WR, Ku JS, Lai JH, Tu CP, Yang CC. J Alloys Compd 2009;483:209.
[10] Zhang C, Zhang F, Chen S, Cao W. JOM 2012;64:7.
[11] Inoue, A, Acta Mater 2000;48:279.
[12] Mizutani U. *Hume-Rothery Rules for Structurally Complex Alloy Phases* (CRC Press, Boca Raton, 2011).
[13] Guo S, Liu CT. Progress in Natural Science: Materials International 2011;21:433.
[14] Teatum,E, Gschneidner,K, Waber,J. (1960) Compilation of calculated data useful in predicting metallurgical behaviour of the elements in binary alloy systems, LA-2345, Los Alamos Scientific Laboratory.
[15] Mann JB, Meek TL, Leland C, Allen LC. J. Am Chem Soc 2000;122:2780.
[16] Mann JB, Meek TL, Knight ET, Capitani JF, Allen LC. J. Am Chem Soc 2000;122:5132.
[17] Guo S, Ng C, Lu J, Liu CT. J Appl Phys 2011;109:103505.
[18] Pettifor DG. Phys Rev Letter 1978;42:846.
[19] Tsai MH, Tsai KY, Tsai CW, Lee C, Juan CC, Yeh JW. Materials Research Letters 2013;1:207.
[20] Turchanin MA, Agraval PG. Powder Metall Met Ceram 2008,47:26.
[21] Harrison W. *Elementary Electronic Structure.* (World Scientific Publishing Co. Pte. Ltd. 2004).
[22] Moriarty JA. Phys Rev 1982;B26:1754.
[23] Pettifor DG. J Phys: Solid St Phys 1970;3:367.
[24] Senkov ON, Wilks GB, Miracle DB, Chuang CP, Liaw PK. Intermetallics 2010;18:1758.
[25] Senkov ON, Scotta JM, Senkova SV, Miracle DB, Woodward CF. J. Alloys Compd 2013; 509:6043.
[26] Yang X, Zhang Y, Liaw PK. Procedia Engineering 2012;36:292.
[27] Hu ZH, Zhan YZ, Zhang GH, She J, Li CH. Mater Des 2010;31:1599.
[28] Zhang Y, Zhou YJ, Lin JP, Chen GL, Liaw PK. Adv Eng Mat 2008;10: 534.
[29] Chang HW, Huang PK, Davison A, Yeh JW, Tsau CH, Yang CC. Thin Solid Films 2008;516:6402.
[30] Zhu JM, Zhang HF, Fu HM, Wang AM, Li H, Hu ZQ. J Alloys Compd 2010;497 :52.
[31] Hsu CY, Wang WR, Tang WY, Chen SK, Yeh JW. Adv Eng Mater 2010;12:44.

[32] Hsu CY, Sheu TS, Yeh JW, Chen SK. Wear 2010;268:653.
[33] Shun TT, Hung CH, Lee CF. J Alloys Compd 2010;493:105.
[34] Zhou YJ, Zhang Y, Wang YL, Chen GL. Mater Sci Eng A 2007;454:260.
[35] Hsu CY, Yeh JW, Chen SK, Shun TT. Metall Mater Trans A 2004;35:1465.
[36] Chou YL, Yeh JW, Shih HC. Corros Sci 2010;52:2571.
[37] Li C, Li JC, Zhao M, Jiang Q. J Alloys Compd 2009;475:752.
[38] Wang XF, Zhang Y, Qiao Y, Chen GL. Intermetallics 2007;15:357.
[39] Li BS, Wang YR, Ren MX, Yang C, Fu HZ. Mater Sci Eng A 2008;498:482.
[40] Varalakshmi S, Kamaraj M, Murty BS. Mater Sci Eng A 2010;527:1027.
[41] Ren B, Liu ZX, Li DM, Shi L, Cai B, Wang MX. J Alloys Compd 2010;493:148.
[42] Chen MR, Lin SJ, Yeh JW, Chuang MH, Chen SK, Huang YS. Metall. Mater. Trans. A 2006;37:1363.
[43] Chou HP, Chang YS, Chen SK, Yeh JW, Mater Sci Eng B 2009;163:184.
[44] Hsu YJ, Chiang WC, Wu JK. Mater Chem Phys 2005;92:112.
[45] Zhou YJ, Zhang Y, Wang FJ, Wang YL, Chen GL. J. Alloys Compd 2008;466 :201.
[46] Chen MR, Lin SJ, Yeh JW; Chen SK, , Huang YS, Tu CP. Mater Trans 2006;47:1395.
[47] Zhou YJ, Zhang Y, Wang FJ, Chen GL. Appl Phys Lett 2008;92:241917.
[48] Wang FJ, Zhang Y, Chen GL. J Alloys Compd 2009;478:321.
[49] Wang FJ, Zhang Y. Mater Sci Eng A 2008;496:214.
[50] Shun TT, Hung CH, Lee CF. J Alloys Compd 2010;495:55.
[51] Zhou YJ, Zhang Y, Wang YL, Chen GL. Appl Phys Let 2007;90:181904.
[52] Chen M, Liu Y, Li YX, Chen X. Acta Metallurgica Sinica 2007;43;1020.
[53] Yeh JW, Chang SY, Hong YD, Chen SK, Lin SJ. Mater Chem Phys 2007;103: 41.
[54] Yeh JW, Lin SJ, Chin TS, Gan JY, Chen SK, Shun TT, Tsau CH, Chou SY. Metall Mater Trans A 2004;35:2533.
[55] Chen HY, Tsai CW, Tung CC, Yeh JW, Shun TT, Yang CC, Chen SK. An. Chim Sci Mat 2006;31:685.
[56] Tung CC, Yeh JW, Shun TT, Chen SK, Huang YS, Chen HC. Materials Letters 2007;61:1.
[57] Tong CJ, Chen YL, Chen SK, Shun TT, Tsau CH, Lin SJ, Chang SY. Metall Mater Trans A 2005;36:881.
[58] Wu WH, Yang CC, Yeh JW. Ann. Chim Sci Mat 2006;31:737.
[59] Zhou YJ, Zhang Y, Wang YL, Chen GL. Appl Phys Lett 2007;5: 181904.
[60] Wen LH, Kou HC, Li JS, Chang H, Xue XY, Zhou L. Intermetallics 2009;17:266.
[61] Ma LQ, Wang LM, Zhang T, Inoue A, Mater Trans JIM 2002;43:277.
[62] Varalakshmi S, Kamaraj M, Murty BS. J Alloys Compd 2008;460:253.
[63] Senkov ON, Senkova SV, Woodward C, Miracle DB. Acta Mater 2013;61:1545.
[64] Liu L, Zhu JB, Zhang C, Li JC, Jiang Q. Mater Sci Eng A 2012;548:64.
[65] Takeuchi A, Inoue A. Mater Trans 2005;46:2817.
[66] Hsu US, Hung UD, Yeh JW, Chen SK, Huang YS, Yang CC.Mater Sci Eng A 2007;460461:403.
[67] de Podesta M. Understanding the Properties of Matter, 2nd edition. London: Taylor Francis, 2002.